Chapter 3

Pipeline Health Monitoring to Optimise Plant Efficiency

Anurag Dhutti and Tat-Hean Gan

Additional information is available at the end of the chapter

http://dx.doi.org/10.5772/intechopen.80844

Abstract

This chapter presents technological innovations that support asset integrity management—a crucial activity for optimising plant efficiency. In ageing thermal and geothermal power plants, critical assets such as steam piping are subject to high pressures and temperatures that accelerate damage mechanisms. Traditionally, the critical locations of these assets undergo routine inspection which is both costly and time consuming and affects the plant reliability and energy availability. There is an increasing trend in the application of non-destructive testing (NDT) and information technologies to in-service monitoring of these assets. The aim of this chapter is to provide a comprehensive overview of the state-of-the-art monitoring technologies for *steamlines*, with a focus on high temperature ultrasonic guided wave techniques. The enabling technologies, which include high temperature sensors, diagnostic data analysis algorithms and their monitoring performances, are reviewed. These technological advancements enable inspection without interruption of plant operations, and provide diagnosis and prognosis data for condition-based maintenance, increasing plant safety and its operational efficiency.

Keywords: thermal power plant, steamlines, non-destructive testing, ultrasonic guided waves, structural health monitoring, temperature compensation, monitoring data analysis, defect detection, optimised maintenance planning

1. Introduction

Thermal power plants (fossil fuel: coal, natural gas, oil; nuclear; and biomass) are critical to the global security of supply, accounting for 80% of global electricity [1], and provide flexibility in capability and availability to meet increasing electricity demand. To remain competitive in emerging utilities markets, the costs of power production need to be reduced. To achieve this, utilities have two key objectives: to reduce capital costs by deferring replacement and life extension of expensive components; and to reduce operating and maintenance (O&M) costs by optimising operations, inspection and maintenance procedures. The need for reduced CO_2 emissions, improved plant efficiency and availability also drives harsher (high process temperatures and pressures) and cyclic duty schedules, resulting in accelerated and severe creep-fatigue damage. This demands increased attention on the critical components. However, reduction of O&M costs may promote fewer, shorter, substandard maintenance and inspection outages, thus placing the critical infrastructure at a greater risk of failure.

In recent years, there has been an increased emphasis on the development of damage prognosis systems that can inform the operators of a structure's health and developing damage, and can provide an estimate of its remaining useful life. These systems have the potential to transform maintenance procedures from schedule-driven to condition-based implementation, thus cutting the time for which the structures are offline, reducing life-cycle costs and decreasing labour requirements. Structural health monitoring (SHM) is an essential component of any damage prognosis system. It allows in-service monitoring of a structure for damage and provides information about any anomalies detected.

This chapter is devoted to high temperature pipelines (HTPs) which are critical components in a thermal power plant (TPP), providing connections between the feed water pumps, the boiler or heat exchanger and the turbine. Each plant has several kilometres of HTP carrying steam under extreme temperature and pressure conditions. At present, the majority of TPPs have an average operating age of over 30 years and HTP failure is listed among the major causes of ageing TPP outages. HTPs suffer continuous cyclic loading and extreme temperature and pressures, and are known to develop defects through a range of mechanisms—creep, fatigue [2], creep-fatigue [3] and thermal fatigue [4], and corrosion [5]. Root-cause analyses of super-heated boiler-tube failure [6] indicate thermal shock and differential thermal expansion are also responsible for defect development. High pH values for steam have been reported to cause stress corrosion cracking (SCC) in heat-affected zones (HAZs) [7].

Failure to detect such defects in HTPs have resulted in catastrophic failures (examples in **Figure 1**) every year or two, causing loss of life and widespread power cuts, with environmental damage and negative financial consequences.

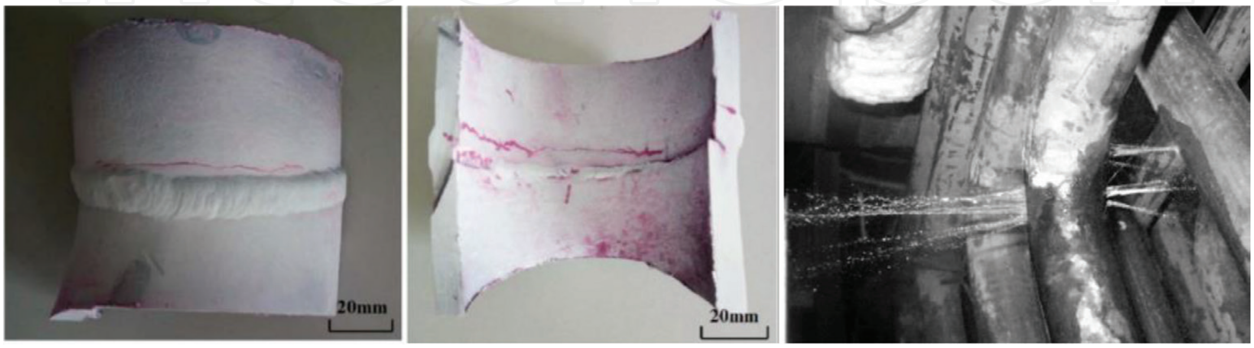

Figure 1. Crack appearance on the outer and inner walls of a furnace tube [7].

http://dx.doi.org/10.5772/intechopen.80844

High resolution non-destructive testing (NDT) technologies such as X-ray and ultrasonic testing (UT) are state-of-the-art for periodic inspection and can detect cracks and wall thickness reduction. These techniques, however, present many challenges, such as over-heating equipment, personnel risks of heat exhaustion or burns, and the difficulty of accessing the pipe surfaces and are therefore only employed during planned maintenance outages. These traditional NDT techniques can provide only local condition information and thus require access to the pipe by, e.g., erection of kilometres of scaffolding and extensive lagging removal, which is expensive and time consuming. The guided wave testing (GWT) approach, on the other hand, provides a non-invasive remote solution with the ability to screen long lengths of pipe and provides 100% cross section area coverage from a single test point; it is also ideal for road crossings and buried pipes. GWT has been widely adopted by the Oil and Gas Industry and, until recently, this approach was used periodically for routine off-load inspections with re-deployable, detachable sensor systems. Repeated access to pipes for re-deployment, however, can be costly and time-consuming, and only possible for HTPs during outages. There are many current commercial systems (for example, see [8, 9]) used in the Oil & Gas Industry, but their operational temperature limits prevent their use on HTP.

This chapter first describes the underlining background of guided wave testing and its influence by temperature. Then recent developments on high temperature transducer design, coupling and data analytics relevant for the application will be discussed. The chapter can serve to provide guidelines for future developments of GWT-based SHM systems for HTP.

2. Background of ultrasonic guided wave technology

2.1. Ultrasonic wave theory

The term "ultrasound" refers to the propagation of mechanical stress waves in a medium at frequencies above 20 kHz, i.e. above the human audible range. Like any other wave, these waves have a velocity (c), wavelength (λ) and frequency (f) which are defined by Filipczynski [10] and related by Eq. (1).

$$c = f\lambda \tag{1}$$

An infinite medium supports two possible wave modes: compression and shear. The particle displacement for these wave modes and the direction of propagation are shown in **Figure 2**.

Compression waves are made up of particles vibrating in the same direction as the propagation of the wave. They can propagate in solids, liquids and gases. Shear (also known as transverse) waves vibrate perpendicular to the direction of propagation and can exist only in materials with shear "stiffness" (solids and viscous liquids). Compression and shear waves travel at different velocities but are constant in most materials at a constant temperature. The propagation velocities of compression waves (c_c) and shear waves (c_s) are related to the material's density (ρ), Poisson ratio (μ) and Young's modulus (E) or the modulus of rigidity (G) by Eq. (2, 3).

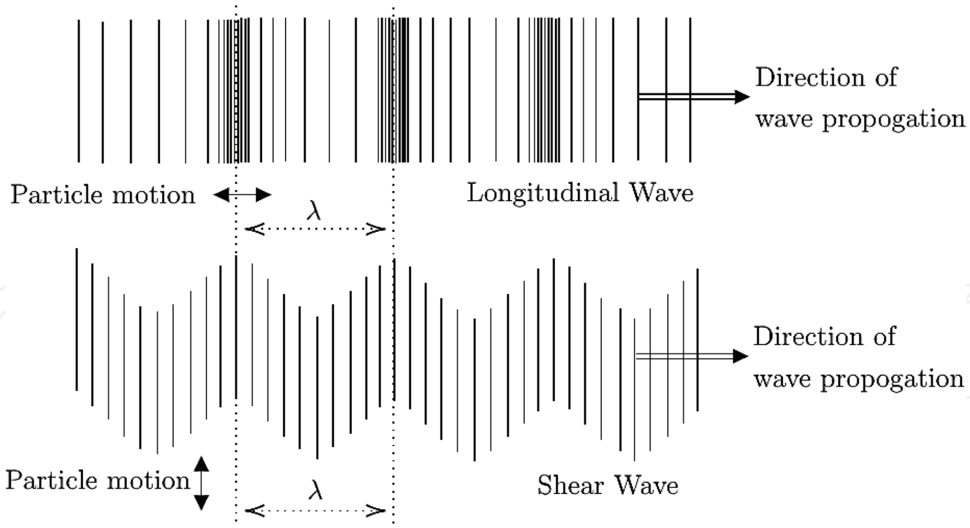

Figure 2. Illustration of particle motion in the two bulk wave modes: longitudinal and shear.

$$C_c = \sqrt{\frac{E(1-\mu)}{\rho(1+\mu)(1-2\mu)}} \tag{2}$$

$$C_s = \sqrt{\frac{E}{2\rho(1+\mu)}} = \sqrt{\frac{G}{\rho}} \tag{3}$$

Acoustic impedance (Z) is used to calculate the reflection and transmission coefficients between two media and is defined as the product of wave velocity (c) and material density (ρ).

$$Z = \rho c \tag{4}$$

Transmission through a finite layer is dependent on the layer's thickness, acoustic impedance and the frequency of the wave. Layers can be acoustically transparent when their thickness is equal to an integral multiple of half wavelengths; due to the formation of standing waves within the layer. This holds when the incident wave is perpendicular to the surface. When the wavelength is much larger than the thickness of the layer, both sides of the layer are approximately in phase so the layer is effectively transparent and these bulk waves travel through a material unaffected by boundaries. Waves that travel along the layers instead of through them are called ultrasonic guided waves (UGW).

Other wave modes such as Rayleigh waves [11] occur due to object boundaries. Rayleigh waves have an elliptical vibration with the major axis of vibration perpendicular to the direction of propagation. These surface waves exist in a half-space, a surface backed by a semi-infinite volume, and can penetrate to a 1.5λ depth below the surface. In contrast, Lamb waves fill the entire volume, provided its thickness is less than 2λ. These were first analysed on plates by Horace Lamb [12] and can be considered as Rayleigh waves bounded by two parallel edges. The fundamental theory of Lamb waves and a review of their applications for long-range inspection of different structures have been reviewed [13].

Just as with plates, hollow tubes have a thin cross section and are bounded by two surfaces. Guided waves in hollow cylinders and thin walled tubes have thus been explored [14] and are also termed Lamb waves. Lamb wave theory assumes an infinite rectangular plate as the medium, but in a hollow cylinder, the circumferential curvature results in a continuous (periodic) boundary condition in distinction to a plate's infinite edge. Therefore the propagation of Lamb waves in tubes is more complex and exists in more numerous modes in tubes than in plates. These will be described in the next section.

2.2. Guided waves in pipes

Guided wave propagation in cylindrical structures has been thoroughly investigated by Gazis and Zemanek [15, 16] who showed the presence of three basic families based on their displacement patterns: Axially symmetric wave modes—longitudinal (L) and torsional (T); and non-axially symmetric—flexural (F) modes, as illustrated in **Figure 3**.

Looking along the pipe from one end, the L wave mode can be visualised as a travelling bulge, the F wave as a flexing of the pipe in any number of directions and the T wave as a twisting of the pipe. The wave modes' designations defined by Meitzler [17] include two numbers, for example, T(0, 1), where the first number is the circumferential wavenumber (also known as the order) and the second number denotes the sequential mode. If the order is zero the wave is axially symmetric and the displacement pattern does not vary around the circumference. All torsional and longitudinal wave modes are axially symmetric. If the order is higher than zero, the wave is non-axially symmetric and must be flexural.

The guided wave particle displacement, u (and particle velocity) is a function of frequency, material thickness and the diameter of the pipe with the following relation in Eq. (5) [18].

$$u = A\,\mathrm{e}^{\mathrm{i}\left(kz + \frac{n\,\theta}{2\,\pi} \omega\, t\right)} \tag{5}$$

where A is a constant, k is the wavenumber along the axis of the pipe, z is the distance along the pipe, n is the wavenumber around the circumference of the pipe and θ is the angle around

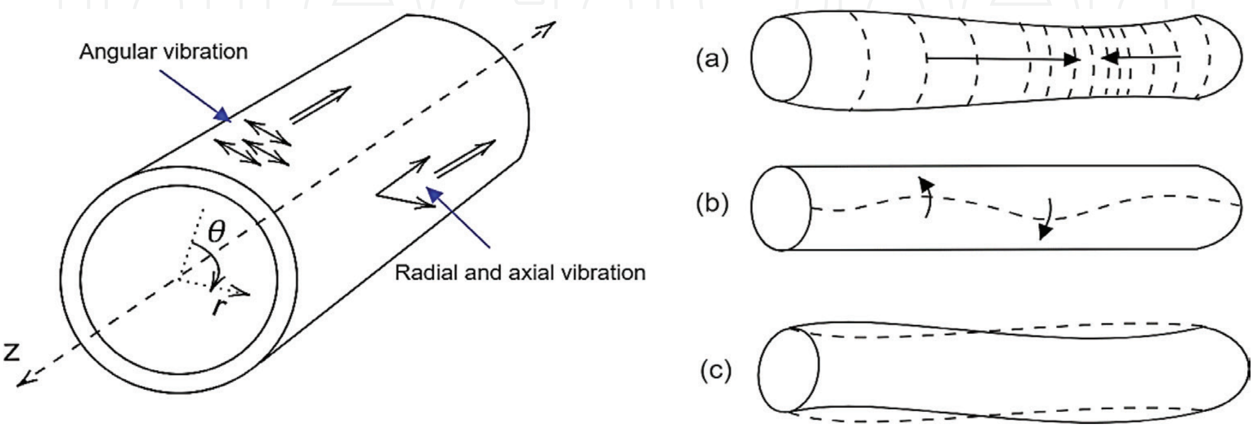

Figure 3. Representation of (a) longitudinal, L (b) torsional, T and (c) flexural, F wave modes in pipes.

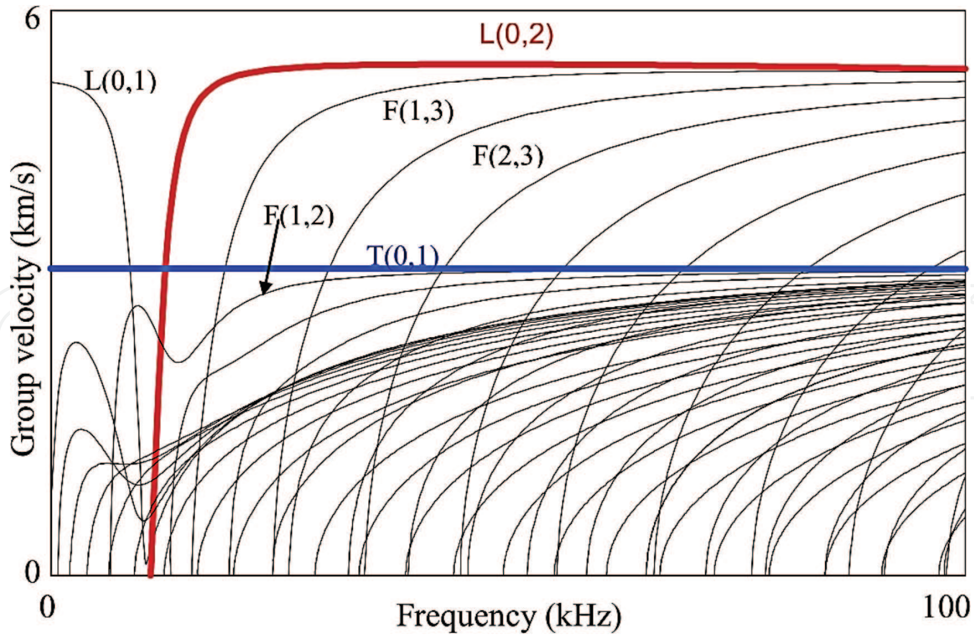

Figure 4. Group velocity dispersion curves for a 6″ schedule *40 steel pipe* [23].

the circumference as defined in **Figure 3**. There are a number of wave modes present at any given frequency. These wave modes can also be described mathematically by the characteristic equation, Eq. (5). The solution of the characteristic equation then provides dispersion curves which are used to illustrate the variation in the wave's phase velocity (v_p) and group velocity (v_g) over a range of frequencies for each wave mode. Commercial software such as *DISPERSE* [19] and *GUIGUW* [20] solve the characteristic equation through iterative computation to generate dispersion curves for multilayer structures.

The group velocity dispersion curve of a 6 inch Schedule 40 steel pipe (**Figure 4**) shows that more than 50 wave modes exist below 100 kHz. For non-dispersive wave modes in a particular frequency range, the phase velocity dispersion curve will be flat with v_p close to v_g [21]. In contrast, dispersive wave modes spread in space over time as they have frequency-dependent velocities and different v_p and v_g. Non-dispersive signals are preferred for ultrasonic testing as dispersion complicates the analysis of signals for flight measurement [22] and reduces the signal to noise ratio. In **Figure 4**, the highlighted fundamental torsional T(0,1) and longitudinal L(0,2) modes are non-dispersive in the frequency range of interest for UGW. These wave modes have been implemented for GWT technique, which will be described now.

2.3. Pipeline inspection using guided wave testing

In conventional UT, high frequency ultrasound is used to measure wall thickness examining the volume of material directly under the test probe location. In contrast, in GWT, an ultrasonic pulse is transmitted along the pipelines via a pulse-echo system (**Figure 5**) which comprises of a pulser-receiver, a laptop PC to control the test and an array of transducers designed to transmit the desired wave mode. Guided waves within pipelines at lower frequencies possess low attenuation and can propagate long distances (tens of meters in each direction). A proportion

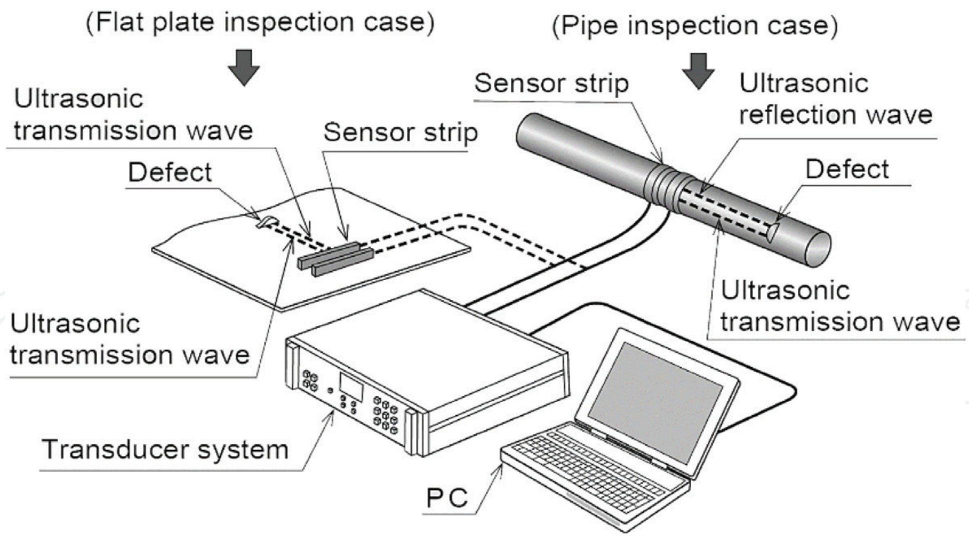

Figure 5. Schematic of guided wave pipe inspection and monitoring system [25].

of the energy contained in the propagating wave front will be reflected back to the tool when an acoustic impedance change occurs due to the presence of a feature or discontinuity in the pipe. It can provide 100% coverage of the cross section of the pipe; detecting and locating both internal and external defects without disrupting operation.

This technology enables rapid screening of long lengths of pipes and is also commonly known as long range ultrasonic testing (LRUT). The definitions and standards for LRUT instrumentation, data collection and analysis have been set in the International Standard ISO 18211:2016 "Nondestructive testing—Long-range inspection of above-ground pipelines and plant piping using guided wave testing with axial propagation" [24].

Initial field trials of this technique were carried out in the mid-1990s [26] where a dry coupled transducer system [27] was used to excite L(0,m) mode and propagation distances approaching 50 m were reported. The same research group began to refine previous findings through their development of a shear transducer and details on responses from a variety of discontinuities found in industrial pipework were reported [28]. This led to the development of several commercial GWT systems [8, 9] which were widely adopted by the Oil and Gas Industry for periodic off-load inspections and have shown reliable defect detection capability for (reducing) defects that remove around 3–9% of the pipe cross section area.

2.3.1. Guided wave mode selection

Dispersion and multiple guided wave modes are the main problems for GWT [29] and excitation of single and non-dispersive wave mode is of practical importance [30] to obtain signals that can be reliably interpreted. The selection of guided wave mode and frequency for GWT depends on properties of the system under inspection (dispersion, attenuation, and sensitivity) and on the transduction system (excitability, detectability and selectivity). Based on these properties, a procedure for identification of suitable modes for a particular inspection task was proposed by Wilcox [31]. T(0,1) and L(0,2) modes are the most attractive modes for GWT as they are non-dispersive and their mode shape has uniform stress over the whole cross section of the pipe providing 100% coverage.

In GWT, the sensitivity is a function of the signal-to-coherent-noise ratio where the coherent noise is caused by excitation of unwanted modes. It is therefore essential to design the transducer system to excite only the chosen mode. Longitudinal modes may provide ~2.5 times more flaw sensitivity compared to torsional modes [32] but complex signal processing is required due to their dispersive nature. In practice, the torsional mode is more commonly used as it is non-dispersive in the entire frequency range, it does not get influenced by fluid in the pipe unlike longitudinal modes (due to their radial displacement) and is also easier to excite in pure form, which will be described in the next section.

2.3.2. Guided wave excitation

There are several transduction technologies for generation and detection of UGW including electromagnetic acoustic transducers (EMATs) [33], piezocomposite transducers, magnetostrictive devices [34], lasers and the most commercially used piezoelectric transducers. A transducer can excite all the modes that exist within its frequency bandwidth. This can complicate signals and make their interpretation difficult.

Initial development of a piezoelectric transducer system for GWT of pipes [26] reported the use of two circumferential rings of dry coupled shear transducer [27] to obtain unidirectional propagation of L(0,2) mode. The directionality is achieved with the application of time delays and phase manipulation between the rings. However, the second axially symmetric L(0,1) mode is also excited by the two-ring system and can make interpretation of the results less reliable. Additional rings of transducers can be implemented to supress the L(0,1) mode but this adds to the cost of the system, especially for larger diameter pipes. Longitudinal modes are also affected by the fluid in the pipe because of their radial displacement.

The T(0,1) mode, on the other hand, is the only axially symmetric torsional mode in the frequency range of interest. So only two rings of transducers are required to obtain single mode and unidirectional excitation. Torsional forcing can be achieved by simply rotating the shear transducer used for the L(0,2) mode by 90° to apply the force in the circumferential direction rather than axially. A transducer array with an even circumferential spacing between transducers generates signals with high-level mode purity. To cancel the propagation of non-axisymmetric Flexural modes, the number of transducers in the ring should be greater than the highest order of flexural mode present in the chosen frequency range [35].

In terms of excitation input, narrow band signals are generally used, such as several cycles of sine wave modulated with a window function (e.g. Hanning). They provide good signal strength and avoid dispersion while propagating long distances. The choice of central frequency for this excitation is based on the desired mode which should have low dispersion over this narrow band so that all frequencies will travel at the same velocity, minimising errors introduced by dispersion. By exciting all transducers in a ring equally and concurrently, an axially symmetric mode is launched.

2.3.3. Guided wave propagation and reflections

When an axisymmetric mode (T or L) is incident on an axisymmetric feature such as a flange, uniform weld or a square end, axisymmetric modes are reflected. But in the presence of non-axisymmetric features such as corrosion, a non-axisymmetric wave will be reflected back to the transducer rings. A number of studies have explored the interaction of UGW modes with defects [35] and features in pipes such as flanges and pipe supports [28]. For the L(0,2) mode the reflection from defects has been evaluated as a function of defect depth, axial and circumferential extent and of excitation frequency [36]. Likewise the interaction of the T(0,1) mode with pipe defects [37] such as cracks and notches [38] and holes [39]. The presence and axial locations of defects can thus be determined by analysing these reflections and their time of arrival.

2.4. Pipeline monitoring system requirements

SHM using GWT has found a variety of practical applications on the rail, ship hull, aircraft and containment structures [40] and the requirement for continuously assessing the integrity of critical pipelines has fostered activities to develop their monitoring systems. A state-of-the-art review of pipe monitoring technologies can be found in [41] but these are not targeted for HTP. There are pipe monitoring solutions for HTP offered by Ionix [42] and Permasense [43] used for wall thickness monitoring but can only provide local coverage at the installed location. To enable long range inspection using GWT for SHM of pipelines, there is a requirement for permanently installed transducers to repeatedly transmit excitation signals and receive responses which are then analysed for early detection of defects to ensure the integrity of the pipeline. The system should be reliable throughout prolonged exposure to variable environmental and operational conditions. A monitoring solution based on GWT-gPIMS [44] is offered by Guided Ultrasonic Ltd. and its stability and defect detection capabilities have been demonstrated [45]. This is however limited to operate at temperatures below 90°C and hence not applicable for HTPs. The following sections review HT transducer designs and the data analysis for temperature corrections that can enable the application to HTPs.

3. High temperature guided wave transducers

3.1. Piezoelectric transducer design

Piezoelectric sensing is the most promising technique due to its high-temperature stability and reliability, and its cost-effectiveness with simple and light-weight construction [46]. Piezoelectric transducers are constructed using five main components: a face plate, a piezoelectric element, backing/damping block, casing and electrical connections, as illustrated in **Figure 6**.

The electrical connection allows the transfer of an electrical pulse to and from the piezoelectric element. The live connection is generally made with a lead, and earthing is effected via the casing. The casing also provides mechanical support for the whole transducer as well as electrical shielding for the piezoelectric element. The damping or backing block damps the vibration

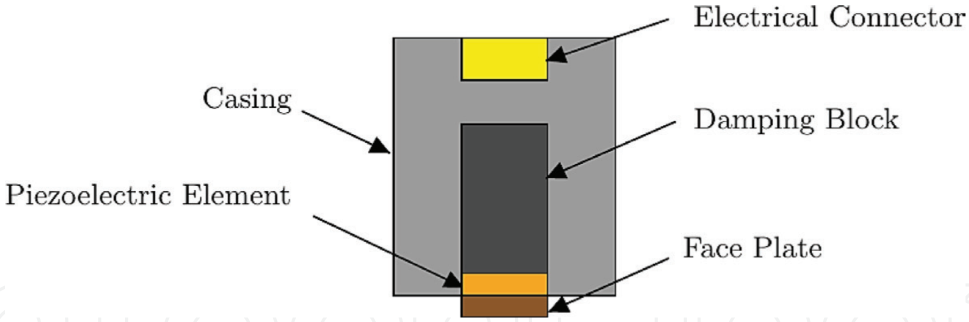

Figure 6. Construction of a generic piezoelectric transducer.

of the piezoelectric element after the excitation pulse has been transmitted. The piezoelectric element generates the mechanical signal from an electrical input—or, conversely, an electrical signal from a mechanical input—enabling transmission and reception of ultrasonic signals, respectively. The face-plate protects the fragile piezoelectric element.

In order to properly design a piezoelectric transducer the following factors must be addressed: (a) all wave modes apart from the one being used for inspection must be suppressed; (b) frequency response should be linear (**Figure 7**) in the region of operation (otherwise neighbouring resonant frequencies may give rise to mode coupling, frequency jumps and performance dips); and (c) the transducer efficiency must be high.

The major challenge for ultrasonic testing at high temperature is to develop transducers that can operate at the target temperatures whilst providing suitable coupling between the transducer and the target material, and provide long term stable performance at the target temperature. This application requires careful selection of materials as presented below.

3.2. High temperature piezoelectric materials

The electromechanical properties that characterise piezoelectric materials are described by a number of interrelated coefficients standardised by the IEEE [47]. These coefficients include

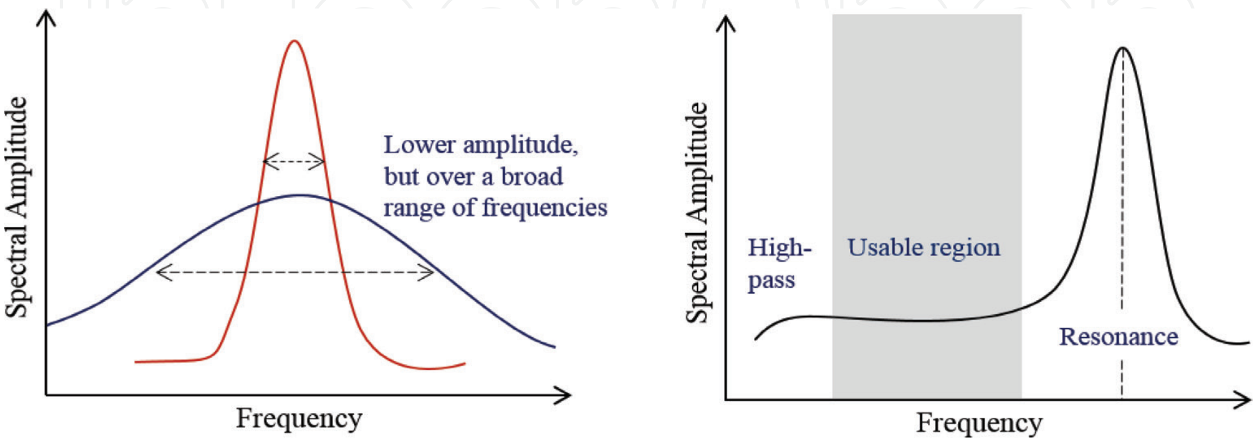

Figure 7. Sketch of a piezoelectric transducer frequency response of a narrow-band (red) and a broadband transducer (blue) (left) and the highlighted region (right) shows the usable region for UGW.

piezoelectric, dielectric and elastic material properties. High temperature piezoelectric materials are being developed for SHM and NDE of the new generation turbines and critical structures in more efficient nuclear/electrical power plants. The temperature limitation of the piezoelectric materials is governed by increased conductivity and mechanical attenuation and variation of the piezoelectric properties with temperature.

There are a number of high temperature materials commercially available and others under development. These are of two types: ferroelectric polycrystalline (such as barium titanate—$BaTiO_3$ and lead zirconate titanate—PZT) and single crystals (such as Quartz—SiO_2 and Lithium Niobate—$LiNbO_3$). The single crystals have high electrical resistivity and low losses, they avoid domain-related ageing behaviour and have an excellent thermal stability. Various piezoelectric materials have been researched for high temperature applications, including quartz, gallium phosphate ($GaPO_4$), langasite ($La_3Ga_5SiO_{14}$), and aluminium nitride (AlN). Each of these materials has unique advantages and drawbacks for use in HTPE transducers and a detailed review of these materials with their properties can be found in [48–50].

A useful guide for the selection of the appropriate piezoelectric material is its figure-of-merit (FOM) depending on the specific application [51]. The FOM for a high temperature transducer is the product of piezoelectric charge and voltage coefficients ($d_{ij} \times g_{ij}$), where a higher value gives a higher electromechanical coupling defining the ratio of stored electrical energy to applied mechanical energy, and *vice versa*. Phase transitions are also an important consideration for material selection, as, beyond specific temperatures, the ferroelectric material may transform from its ferroelectric phase to a high symmetry non-ferroelectric phase. The transition temperature is also referred to as the Curie temperature (T_c) and above this temperature, the material is permanently depolarized and no longer piezoelectric. For high temperature monitoring applications, it is not recommended to use ferroelectric materials at temperatures exceeding $0.5T_c$ [52] in order to minimise thermal ageing and property degradation. **Figure 8** shows the FOM of selected piezoelectric materials for high temperature shear transducer.

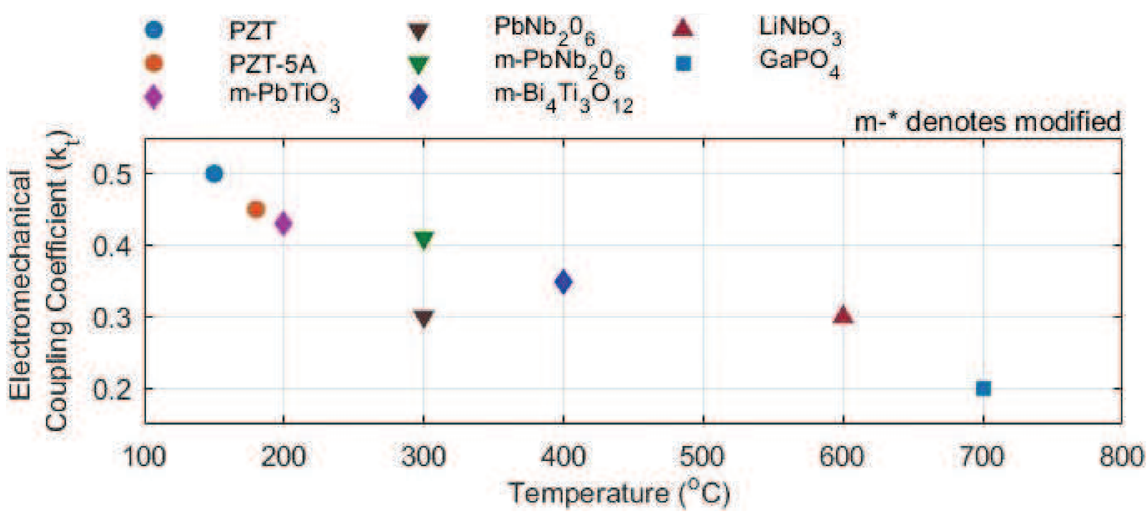

Figure 8. High temperature piezoelectric materials and their maximum operating temperature and electromechanical coupling factor in the thickness mode.

To apply the electric field and to obtain the generated charge signal in the piezoelectric material, thin film electrodes (~100 nm) are commonly applied. Many metallic, metallic alloys and conductive ceramic electrodes have been researched for high temperature applications. The most popular is a platinum thin film electrode (recommended for T < 650°C) with persisting excellent electrical properties, high melting point and resistance to oxidation. Other thin film electrodes for operation at temperatures up to 850°C have been summarised in [53]. The shape of the electrode can also influence the behaviour or mode of vibration as shown in a previous study [54], so FEA modelling is often necessary to achieve the desired displacement patterns.

3.3. High temperature transducer backing

In contrast to bulk resonant transducers which have relatively low internal damping making them very good for producing resonant transducers, piezoelectric materials must be damped heavily to produce broadband, guided-wave transducers.

3.4. Transducer assembly for high temperatures

To assemble the transducer the components in Section 3.1 must be bonded together. There are limitations on how this can be done without damaging the parts—particularly the piezoelectric material. The temperature required for bonding must not be high enough to cause melting and must be below half of the piezoelectric material's Curie temperature. The bond must also remain strong at the operating temperature of the device, as the transducer assembly can suffer permanent damage at high temperatures caused by excessive differential thermal expansion. The pressure used in the bonding process is another key parameter—at too high a pressure there could be damage to the parts. A crack on one part will cause diffraction of the acoustic waves which could seriously affect the performance of the transducer. The bond must also be elastic in order to be able to change shape as the piezoelectric deforms, and as the other parts of the transducer expand or contract due to changes in temperature. Common methods of bonding include the use of high temperature epoxy, which is a thermosetting polymer used as a glue. Also, glass solder can be used up to 500°C, after which it reacts chemically with other components. Other methods include regular soldering, diffusion bonding, ultrasonic welding, cementing, sol–gel and vacuum brazing. A comprehensive review of these bonding techniques and designs of ultrasonic transducers for high temperature can be found in [48].

3.5. Transducer coupling mechanism

The mechanical wave generated within the piezoelectric element has to be coupled into the object to be inspected. There are three different methods of acoustic coupling at high temperatures: dry-coupling (with a high pressure); fluid coupling; and solid coupling. For high frequency UT, the ultrasound propagates through the transducer's face plate to the object through a couplant, generally a gel but an elastomer or water can also be used. However, for UGW shear wave transducers, a coupling with a high modulus of rigidity must be used, which is commonly achieved by dry-coupling. The piezoelectric transducers may be attached to the pipe using adhesives. The effect of adhesive on the ultrasonic vibrations has been investigated through parametric studies on bonding layer properties such as adhesive thickness and shear modulus [55]. Improperly prepared bonding layers with uneven distribution of adhesives under the transducer can significantly reduce the performance of the transducer. Two methods—electromechanical impedance characterisation and time-domain terahertz spectroscopy [56]—have been previously used to assess the quality of these adhesive bond.

4. Guided wave monitoring data analysis

Once the SHM system is installed on the pipe, regular inspection data is recorded into a monitoring database. The collected UGW data is then processed to provide information regarding the presence of a defect and information regarding its type, location and severity. The performance of defect detection techniques relies on the hypothesis that the recorded signal remains stable if no defect is present. The UGW data is, however, susceptible to changes in environmental and operational conditions (EOCs) such as temperature, humidity, pressure, vibration, flow, etc., influencing the electronic devices, transducer time behaviour and even the structure itself. Of the EOCs, temperature has been shown to be the dominant effect on UGW, often masking the real damage information. This can lead to false diagnostics and prognostics and therefore to ensure the reliability of the SHM system, the data should be corrected for any temperature induced variations. In the following sections, the effect of temperature on the UGW signals will be described and different data correction methodologies are discussed. Thereafter, approaches for defect detection from the corrected data are presented.

4.1. Effect of temperature on ultrasonic guided waves

Propagation of sound depends on the type, temperature and composition of the medium. Several investigations into the effect of temperature on the recorded waveform have been carried out [57] and change of temperature has been shown to be the main source of fluctuations in the received signals [58]. The influence of temperature on GWT of pipes is a combination of effects on the pipe mechanical properties and on ultrasonic transducers and their bonding [59]. However, for small temperature variations of a few degrees, the effect on transducer performance has been shown to be significantly less than that on wave propagation [60].

UGW signals undergo changes in amplitude and phase under the influence of varying temperature. The phase shift in the transducer signals is mainly attributable to the change in wave propagation velocity from changes in the mechanical properties of the pipe [61]. Changes in signal amplitude are attributable to changes in the temperature-dependant properties of the ultrasonic transducer, particularly of the piezoelectric and adhesive materials, as described in Section 3. It is possible through careful selection of adhesives and transducer materials to minimise this variability.

The relevant pipe mechanical properties are the elastic and shear moduli and the density, which relate to the elasto-acoustic properties of the material, acoustical absorption and ultrasonic wave velocity. Thermal expansion changes propagation distance directly and indirectly through changes in the thickness of the pipe. The effects of temperature are also reported to be increased at greater propagation distance. The relationship between the difference in arrival times of the signal and the change in temperature of the structure can be written as

$$\delta t = \frac{d}{v}(\alpha - \gamma)\delta T \tag{6}$$

Here, δt is the difference in arrival times of signals when the change in temperature of the structure is δT. d is the distance propagated by the wave and v is the wave velocity. α is the coefficient of thermal expansion and γ is the coefficient of change in phase velocity. γ is usually significantly greater than α and hence from Eq.(6), it can be seen that the main contribution to the time shift due to temperature variations is from the change in wave velocity. Also, since the time shift is directly proportional to the propagation distance, the effect of temperature variation increases with propagation distance. The inverse relation to the wave velocity suggests that faster modes will be less affected than slower ones.

4.2. Signal processing for data correction

Temperature-induced variations in UGW signals can adversely affect the defect detection capabilities as observed in a previous study [62] which investigated the effect of temperature variation on Lamb waves from ambient temperatures up to 70°C. The temperature effect (analysed using principal components) was reported much more pronounced than the effect of a drilled damage (hole) with a diameter of 1 mm. There have been several investigations within the SHM research community to address this issue, and a number of temperature-compensation strategies have been proposed. The main objective of temperature compensation is to achieve propagation time and amplitude correction, and these strategies can be divided into two techniques: data driven and analytical physics-based.

For data driven techniques, a large baseline set of transducer measurements from the structure at a different temperature is required. It has been suggested to use a 'bank' of baseline signals for various temperatures and to pick a baseline signal which minimises differences relative to the test signal for that temperature. This method is called optimum baseline selection (OBS) and the selection criteria can be based on mean square deviation [57] or maximum residual amplitude [63]. A large baseline set is not always available and in some cases, the temperature of the selected baseline can be different from the temperature of the test signal. In order to adjust the selected baseline, baseline signal stretch (BSS) was introduced, which in its simplest form only requires a single baseline datum at a reference temperature. BSS is carried out using time domain stretching where local coherence is estimated as a function of time using short time cross-correlation [57]. A combination of BSS and OBS has been applied by [59, 63–65] to provide enhanced temperature compensation while requiring a reduced number of baseline data sets. New methodologies proposed for stretch-based temperature compensation [66] operate on signals in the stretch factor and scale-transform domain and have shown improved computation speed.

The physics-based compensation techniques [57, 67] are based on transducer signal reconstruction at different temperatures based on underlying physical principles as described in Section 4.1. One such technique is proposed in [68] where the changes in elastic modulus and thermal expansion were used to model the varying time-of-flight over a modest temperature range within ±50°C, which gave good agreement with experiments. These analytical solutions

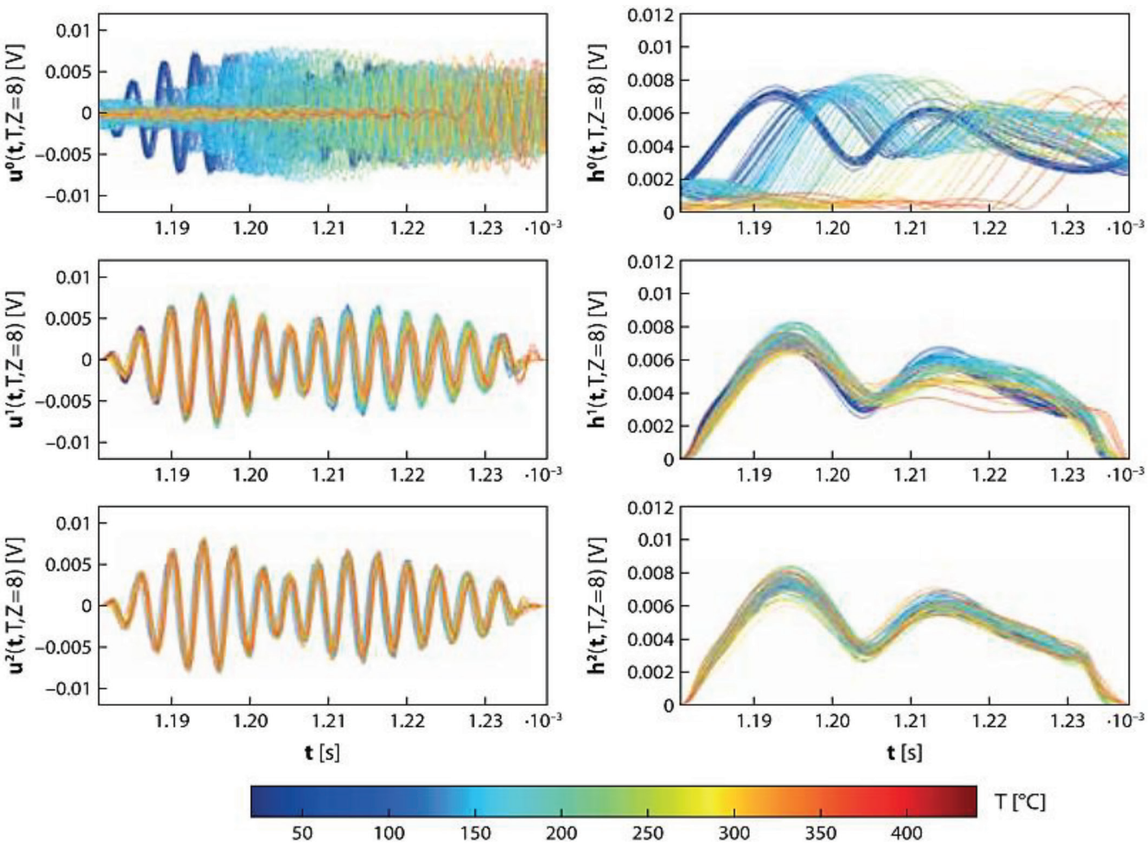

Figure 9. Example results of temperature correction, (top) original signals, signals after (middle) correction in the time domain, and (bottom) phase and amplitude correction [69].

were limited to simple structural geometries and boundary conditions. Analytical models can also be coupled with data-driven strategies, with fewer baseline measurements making this approach efficient, practical and useful (**Figure 9**) as demonstrated in [69].

4.3. Damage detection methodologies

To detect whether the pipeline being inspected has developed damage, a method for damage detection must be applied to the corrected data. Damage detection is generally performed by unsupervised algorithms, as the inspection data corresponding to the damage state is not known *a priori*. One such algorithm is outlier analysis (OA) [70] where damage sensitive features are extracted from the signals, and the aim is to identify if the measured signal has deviated from the baseline distribution by defining a threshold. This threshold depends on the baseline data and its statistical representation. The analysis can be applied as univariate or multivariate depending on the number of features. Root mean square (RMS) value has been successfully used as a damage sensitive feature for detection of notch and hole type defects on a plate [57], and for corrosion type defects on pipes [71] using torsional and flexural modes. For multivariate analysis, a vector of damage index is formed by extracting a number of features and classical methods of multi-variate statistics such as principal component analysis (PCA) is applied to them. For the multi-variate case, OA can be performed using a self-organising mapping technique [72] or Mahalanobis squared distance [70]. An artificial neural network (ANN) based method was applied in [70] for damage classification and it was able to outperform OA for damage detection with just one feature. However, for implementing an ANN based approach, data from the structure with known types and levels of damage is required.

5. Conclusions

This chapter presents GWT for structural health monitoring of high temperature pipelines to support asset integrity management and condition based maintenance for optimising plant efficiency. To provide the reader with a background on GWT, a comprehensive overview of this technology covered the fundamental theory of guided waves in pipes, GWT system components and the desired input parameters for optimising performance. GWT technology has been widely used in the industry for routine inspection of pipelines. To avoid costs associated with repeated access, monitoring systems have been developed and have demonstrated the improved reliability of information and enhanced defect detection capability. The enabling technologies for HTP monitoring, which include high temperature guided wave transducers, temperature data correction and diagnostic algorithms, are reviewed. These technologies can advance the current GWT-based monitoring systems for application on HTPs. This will provide diagnosis and prognosis data to ensure the integrity of HTPs without interruption of plant operation, thus increasing plant safety and its operational efficiency.

Author details

Anurag Dhutti[1] and Tat-Hean Gan[1,2]*

*Address all correspondence to: tat-hean.gan@brunel.ac.uk

1 Brunel University London, UK

2 TWI Ltd. Granta Park, Cambridge, UK

References

[1] International Energy Agency. Key world energy statistics [Internet]. 2017. Available from: http://www.iea.org/ [Accessed: 02/01/2018]

[2] Bush SH. Failure mechanisms in nuclear power plant piping systems. Journal of Pressure Vessel Technology. 1992;**114**:389-396. DOI: 10.1115/1.2929244

[3] Gaur B, Babakr A. Piping failure in a superheated steam service—A case study. Matériaux & Techniques. 2013;**101**:206. DOI: 10.1051/mattech/2013067

[4] Viswanathan R, Stringer J. Failure mechanisms of high temperature components in power plants. Journal of Engineering Materials and Technology. 2000;**122**:246-255. DOI: 10.1115/1.482794

[5] Sabouri M, Hoseiny H, Faridi HR. Corrosion failure of superheat steam pipes of an ammonia production plant. Vacuum. 2015;**121**:75-80. DOI: 10.1016/j.vacuum.2015.07.022

[6] Naď M, Buzík J, Létal T, Lošák P. Root-cause analysis of superheater-tube failure. Materials and Technology. 2017;**51**:503-507. DOI: 10.17222/mit.2016.204

[7] Xu S, Meng W, Wang C, Sun Z, Zhang Y. Failure analysis of TP304H tubes in the superheated steam section of a reformer furnace. Engineering Failure Analysis. 2017;**79**: 762-772. DOI: 10.1016/j.engfailanal. 2017.05.033

[8] Eddyfi. Long-Range Guided Wave Testing with Teletest Focus+ [Internet]. 2018. Available from: https://www.teletestndt.com/ [Accessed: 06/10/2018]

[9] Guilded Ultrasonic Ltd. Inspection [Internet]. Available from: http://www.guided-ultrasonics.com/inspection/ [Accessed: 06/10/2018]

[10] Filipczyński L, Pawłowski Z, Wehr J. Ultrasonic Methods of Testing Materials. London, UK: Butterworths; 1966. p. 280

[11] Viktorov IA. Rayleigh and Lamb Waves. Boston, MA: Springer US; 1967. p. 154. DOI: 10.1007/978-1-4899-5681-1

[12] Lamb H. On waves in an elastic plate. Proceedings of the Royal Society A: Mathematical, Physical and Engineering Sciences. 1917;**93**:114-128. DOI: 10.1098/rspa. 1917.0008

[13] Su Z, Ye L. Identification of Damage Using Lamb Waves. London: Springer; 2009. p. 346. DOI: 10.1007/978-1-84882-784-4

[14] Silk MG, Bainton KF. The propagation in metal tubing of ultrasonic wave modes equivalent to lamb waves. Ultrasonics. 1979;**17**:11-19. DOI: 10.1016/0041-624X (79)90006-4

[15] Gazis DC, Herman R, Wallis RF. Surface elastic waves in cubic crystals. Physics Review. 1960;**119**:533-544. DOI: 10.1103/PhysRev.119.533

[16] Zemanek J. An experimental and theoretical investigation of elastic wave propagation in a cylinder. The Journal of the Acoustical Society of America. 1972;**51**:265-283. DOI: 10.1121/1.1912838

[17] Meitzler AH. Mode coupling occurring in the propagation of elastic pulses in wires. The Journal of the Acoustical Society of America. 1961;**33**:435-445. DOI: 10.1121/1.1908685

[18] Gazis DC. Three-dimensional investigation of the propagation of waves in hollow circular cylinders. The Journal of the Acoustical Society of America. 1959;**31**:573-578. DOI: 10.1121/1.1907754

[19] Lowe MJS. A model for predicting the properties of guided ultrasonic waves, and illustration of its application to NDT. In: IEE Colloquium New Applications in Modelling and Inversion Techniques for Non-Destructive Testing. IEE; 1999

[20] Bocchini P, Marzani A, Viola E. Graphical user interface for guided acoustic waves. Journal of Computing in Civil Engineering. 2011;**25**:202-210. DOI: 10.1061/(ASCE)CP.1943-5487. 0000081

[21] Krautkrämer J, Krautkrämer H. Wave Physics of the Sound Field. Berlin Heidelberg: Springer; 1990. pp. 58-92. DOI: 10.1007/978-3-662-10680-8_5

[22] Cawley P, Alleyne D. The use of lamb waves for the long range inspection of large structures. Ultrasonics. 1996;**34**:287-290. DOI: 10.1016/0041-624X (96)00024-8

[23] Lowe MJS, Cawley P. Long range guided wave inspection usage—Current commercial capabilities and research directions. Technical Report, Department of Mechanical Engineering, Imperial College London. 2006. pp.1-40. DOI: 10.1177/058310240

[24] ISO 18211:2016. Non-destructive testing—Long-range inspection of above-ground pipelines and plant piping using guided wave testing with axial propagation. 2016

[25] Kuroishi T, Sakata F. New application of NDE technology guided wave pipe inspection and monitoring system. Journal of The Japan Welding Society. 2006;**75**:220-224. DOI: 10.2207/jjws.75.220

[26] Alleyne DN, Cawley P, Lank AM, Mudge PJ. The lamb wave inspection of chemical plant pipework. In: Review of Progress in Quantitative Nondestructive Evaluation. Boston, MA: Springer US; 1997. pp. 1269-1276

[27] Alleyne DN, Cawley P. The excitation of lamb waves in pipes using dry-coupled piezoelectric transducers. Journal of Non-destructive Evaluation. 1996;**15**:11-20. DOI: 10.1007/BF00733822

[28] Alleyne DN, Cawley P. The effect of discontinuities on the long-range propagation of lamb waves in pipes. Proceedings of the Institution of Mechanical Engineers. 1996;**210**: 217-226. DOI: 10.1243/PIME_PROC_1996_210_316_02

[29] Wilcox P, Lowe M, Cawley P. The effect of dispersion on long-range inspection using guided waves. NDT & E International. 2001;**34**:1-9. DOI: 10.1016/S0963-8695 (00)00024-4

[30] Galvagni A, Cawley P. The reflection of guided waves from simple support in pipes. The Journal of the Acoustical Society of America. 2011;**129**:1869-1880. DOI: 10.1121/1.3543958

[31] Wilcox PD, Lowe MJS, Cawley P. Mode and transducer selection for long range lamb wave inspection. Journal of Intelligent Material Systems and Structures. 2001;**12**:553-565. DOI: 10.1106/N9PB-Y62E-P0Y2-50QF

[32] Lowe PS, Sanderson RM, Boulgouris NV, Haig AG, Balachandran W. Inspection of cylindrical structures using the first longitudinal guided wave mode for higher flaw sensitivity. IEEE Sensors Journal. 2016;**16**:706-714. DOI: 10.1109/JSEN. 2015.2487602

[33] Clough M, Fleming M, Dixon S. Circumferential guided wave EMAT system for pipeline screening using shear horizontal ultrasound. NDT & E International. 2017;**86**:20-27. DOI: 10.1016/j.ndteint.2016.11.010

[34] Zhu L, Wang Y, Sun F. Single torsional guided wave excitation in pipes using magnetostrictive technology. In: 2013 IEEE 11th International Conference on Electronic Measurement & Instruments, ICEMI 2013. Vol. 2. 2013. pp. 872-876. DOI: 10.1109/ICEMI.2013.6743158

[35] Lowe MJS, Alleyne DN, Cawley P. Defect detection in pipes using guided waves. Ultrasonics. 1998;**36**:147-154. DOI: 10.1016/S0041-624X (97)00038-3

[36] Cawley P, Lowe MJS, Simonetti F, Chevalier C, Roosenbrand AG. The variation of the reflection coefficient of extensional guided waves in pipes from defects as a function of defect depth, axial extent, circumferential extent and frequency. Proceedings of the Institution of Mechanical Engineers. 2002:1131-1143. DOI: 10.1243/095440602761609498

[37] Rojas E, Baltazar A, Treesatayapun C. Investigation on damage identification in a pipe using torsional guided waves. In: AIP Conference Proceedings. 2017

[38] Demma A, Cawley P, Lowe M, Roosenbrand AG. The reflection of T(0, 1) mode from cracks and notches in pipes. The Journal of the Acoustical Society of America. 2003;**114**: 611-625. DOI: 10.1121/1.1582439

[39] Løvstad A, Cawley P. The reflection of T(0, 1) guided wave from multiple circular holes in pipes. NDT & E International. 2011;**44**:553-562. DOI: 10.1016/j.ndteint.2011.05.010

[40] Rose JL. Ultrasonic guided waves in structural health monitoring. Key Engineering Materials. 2004;**270-273**:14-21. DOI: 10.4028/www.scientific.net/KEM.270-273.14

[41] Liu Z, Kleiner Y. State-of-the-art review of technologies for pipe structural health monitoring. IEEE Sensors Journal. 2012;**12**:1987-1992. DOI: 10.1109/JSEN. 2011.2181161

[42] Advanced Ionix Technologies. Pipeline corrosion monitoring system [Internet]. Available from: https://ionixadvancedtechnologies.co.uk/ [Accessed: 05/01/2018]

[43] Permasense. Permasense—Experts in remote monitoring solutions [Internet]. 2018. Available from: https://www.permasense.com/ [Accessed: 06/22/2018]

[44] Guided Ultrasonics Ltd. gPIMS [Internet]. Available from: https://www.guided-ultrasonics.com/gpims/ [Accessed: 05/10/2018]

[45] Cawley P, Cegla F, Galvagni A. Guided waves for NDT and permanently-installed monitoring. Insight Non-Destructive Test Cond Monit. 2012;**54**. DOI: 594-601. DOI:10.1784/insi. 2012.54.11.594

[46] Jiang X, Kim K, Zhang S, Johnson J, Salazar G. High-temperature piezoelectric sensing. Sensors (Switzerland). 2013;**14**:144-169. DOI: 10.3390/s140100144

[47] Standards Committee of the IEEE Ultrasonics, Ferroelectrics and FCS. IEEE Standard on Piezoelectricity. Society; 1988. DOI: 10.1109/IEEESTD.1988.79638

[48] Kažys R, Voleišis A, Voleišienė B, Kazys R, Voleisis A, Voleisiene B. High temperature ultrasonic transducers : Review. Ultrasound. 2008;**63**:7-17

[49] Zhang S, Yu F. Piezoelectric materials for high temperature sensors. Journal of the American Ceramic Society. 2011;**94**:3153-3170. DOI: 10.1111/j.1551-2916. 2011.04792.x

[50] Shinekumar K, Dutta S. High-temperature piezoelectrics with large piezoelectric coefficients. Journal of Electronic Materials. 2014;**44**:613-622. DOI: 10.1007/s11664-014-3534-2

[51] Lee H, Zhang S, Bar-Cohen Y, Sherrit S. High temperature, high power piezoelectric composite transducers. Sensors. 2014;**14**:14526-14552. DOI: 10.3390/s140814526

[52] Gotmare SW, Leontsev SO, Eitel RE. Thermal degradation and aging of high-temperature piezoelectric ceramics. Journal of the American Ceramic Society. 2010;**93**:1965-1969. DOI: 10.1111/j.1551-2916.2010.03663.x

[53] Richter D, Sakharov S, Forsén E, Mayer E, Reindl L, Fritze H. Thin film electrodes for high temperature SAW devices. Procedia Engineering. 2011;**25**:168-171. DOI: 10.1016/j.proeng.2011.12.042

[54] Dhutti A, Gan TH, Balachandran W. Effect of electrode configuration on high temperature thickness shear $GaPo_4$ transducer. MDPI Proceedings. 2017;**1**:381-385. DOI: 10.3390/proceedings 1040381

[55] Islam MM, Huang H. Effects of adhesive thickness on the lamb wave pitch-catch signal using bonded piezoelectric wafer transducers. Smart Materials and Structures. 2016;**25**. DOI: 10.1088/0964-1726/25/8/085014

[56] Wandowski T, Moll J, Malinowski P, Ostachowicz W. Assessment of piezoelectric sensor adhesive bonding. Journal of Physics Conference Series. 2015;**628**. DOI: 10.1088/1742-6596/628/1/012114

[57] Lu Y, Michaels JE. A methodology for SHM with diffuse ultrasonic waves in the presence of temperature variations. Ultrasonics. 2005;**43**:717-731. DOI: 10.1016/j.ultras.2005.05.001

[58] Mazzeranghi A, Vangi D. Methodology for minimizing temperature effects in monitoring with acousto-ultrasonic technique. Experimental Mechanics. 1999;**39**:86-91. DOI: 10.1007/BF02331110

[59] Croxford AJJ, Wilcox PDD, Drinkwater BWW, Konstantinidis G. Strategies for guided-wave structural health monitoring. Proceedings of the Royal Society A: Mathematical, Physical and Engineering Science. 2007;**463**:2961-2981. DOI: 10.1098/rspa.2007.0048

[60] Konstantinidis G, Wilcox PD, Drinkwater BW. An investigation into the temperature stability of a guided wave structural health monitoring system using permanently attached sensors. IEEE Sensors Journal. 2007;**7**:905-912. DOI: 10.1109/JSEN.2007.894908

[61] Wilcox PD, Konstantinidis G, Croxford AJ, Drinkwater BW. Strategies for guided wave structural health monitoring. AIP Conference Proceedings. 2007;**894**:1469-1476. DOI: 10.1063/1.2718139

[62] Lee BC, Staszewski WJ. Modelling of lamb waves for damage detection in metallic structures: Part II. Smart Materials and Structures. 2003;**12**:815-824. DOI: 10.1088/0964-1726/12/5/019

[63] Clarke T, Simonetti F, Cawley P. Guided wave health monitoring of complex structures by sparse array systems: Influence of temperature changes on performance. Journal of Sound and Vibration. 2009;**329**:2306-2322. DOI: 10.1016/j.jsv.2009.01.052

[64] Wilcox PD, Croxford AJ, Michaels JE, Lu Y, Drinkwater BW. A comparison of temperature compensation methods for guided wave structural health monitoring. AIP Conference Proceedings. 2008;**975**:1453-1460. DOI: 10.1063/1.2902606

[65] Croxford AJ, Moll J, Wilcox PD, Michaels JE. Efficient temperature compensation strategies for guided wave structural health monitoring. Ultrasonics. 2010;**50**:517-528. DOI: 10.1016/j.ultras.2009.11.002

[66] Harley JB, Moura JMF, Fry FEJ. Scale transform signal processing for optimal ultrasonic temperature compensation. IEEE Transactions on Ultrasonics, Ferroelectrics, and Frequency Control. 2012;**59**:2226-2236. DOI: 10.1146/annurev.ph.20.030158.001231

[67] Konstantinidis G, Drinkwater BW, Wilcox PD. The temperature stability of guided wave SHM systems. Smart Materials and Structures. 2006;**15**:967-976. DOI: 10.1088/0964-1726/15/4/010

[68] Roy S, Lonkar K, Janapati V, Chang F-K. A novel physics-based temperature compensation model for structural health monitoring using ultrasonic guided waves. Structural Health Monitoring. 2014;**13**:321-342. DOI: 10.1177/1475921714522846

[69] Weihnacht B, Klesse T, Neubeck R, Schubert L. Monitoring of hot pipes at the power plant Neurath using guided waves. In: Sensors and Smart Structures Technologies for Civil, Mechanical, and Aerospace Systems. San Diego, CA, USA; 2013

[70] Bagheri A, Pistone E, Rizzo P. Outlier analysis and artificial neural network for the noncontact nondestructive evaluation of immersed plates. Research in Nondestructive Evaluation. 2015;**26**:154-173. DOI: 10.1080/09349847.2015.1022677

[71] Mountassir MEL, Yaacoubi S, Mourot G, Maquin D. Studies on data correction of structural health monitoring using ultrasonic guided waves : Case of study. In: Proceedings 8th EWSHM Conference. Spain: Bilbao; 2016

[72] Buethe I, Mujica L. Damage detection in piping systems using pattern recognition techniques. In: Proceedings 6th EWSHM Conference. Germany: Dresden. p. 2012